Some issues on turbulent mixing and turbulence

Paul E. Dimotakis

Graduate Aeronautical Laboratories
California Institute of Technology
Pasadena, California 91125

Abstract

Recent data on turbulent mixing suggest that the mixing transition, previously documented to occur in shear layers, also occurs in jets, as well as many other flows, and can be regarded as a universal phenomenon. The resulting, fully-developed turbulent flow requires a minimum Reynolds number of $Re \approx 10^4$, or a Taylor Reynolds number of $Re_T \approx 10^2$, to be sustained. Turbulent mixing in this fully-developed state does not appear to be universal, however, with a qualitatively different behavior between shear layers and jets.

Presented at the Turbulence Symposium in honor of W. C. Reynolds' 60$^{\text{th}}$ birthday
22–23 March 1993, Monterey, California

GALCIT Report FM93–1a

17 March 1993

Revised: 6 July 1993

1. Introduction

A correct description of turbulent mixing is particularly taxing on our understanding of turbulence; such a description relies on an account of the full spectrum of scales. Specifically, to describe the *entrainment* stage that is responsible for the engulfment of large pockets of irrotational fluid species into the turbulent flow region,[1] the large scale flow structures need to be correctly described. Secondly, to describe the subsequent kinematic *stirring* process that is responsible for the large interfacial surface generation between the mixing species, the intermediate range of scales must be correctly accounted for. These are below the largest in the flow in size, but above the smallest affected by viscosity and molecular diffusivity. Finally, the dynamics at the smallest scales must be captured to describe the *molecular mixing* process itself. These three phases of turbulent mixing were clearly identified as "more or less distinct stages" in the 1948 description of mixing by Eckart,[2] who dubbed them as the *initial*, *intermediate*, and *final* stages, respectively. In the case of mixing of high Schmidt number fluids, *i.e.*, fluids characterized by a molecular diffusivity, $\mathcal{D}$, that is much smaller than the kinematic viscosity, ν, it is also useful to distinguish between the vorticity-diffusion stage, whereby velocity gradients are removed, and the species-diffusion stage, which removes scalar gradients.[3]

On the other side, successful descriptions and models of mixing provide us with tests of aspects of turbulent flow that are difficult to probe by other means — experimentally, numerically, or theoretically — at the high Reynolds numbers of interest here.

An exciting discussion in the context of mixing by chaotic advection has been taking place during the last decade. See, for example, Refs. 4–7, as well as several papers from the 1990 *IUTAM Symposium on Fluid Mechanics of Stirring and Mixing* (Published in *Phys. Fluids* A **5**, Part 2, May 1991). There is little doubt that this progress will contribute to our understanding in the context of the broader issues of turbulent mixing. The present discussion, however, will be limited to flows at Reynolds numbers that are high enough for the turbulence to be regarded as fully-developed. In that regime, the impact of the recent progress in the behavior of deterministic, chaotic systems has yet to be felt, in my opinion.

As a practical matter, fully-developed turbulent flow typically requires that the local flow Reynolds number, *i.e.*,

$$Re(x) \;=\; \frac{U(x)\,\delta(x)}{\nu} \tag{1}$$

must be high enough. Generally speaking, turbulence cannot be sustained if the (local) Reynolds number falls below some minimum value, $Re_{\min}$. In the expression in Eq. 1, the characteristic velocity, $U(x)$, and transverse extent of the flow, $\delta(x)$, are to be taken as local values.

The main part of the discussion will be drawn from turbulent mixing in the far field of nonaccelerating (negligible streamwise pressure gradient) shear layers and jets. While these two flows are similar, in many ways, they are sufficiently different in others to be useful as test beds of ideas and prospects for universal descriptions of turbulent mixing behavior. The phenomena are found to have a broader manifestation, however, with conclusions relevant to turbulent flow in general.

In the case of shear layers, the characteristic velocity will be taken as the (constant) freestream velocity difference, *i.e.*, $U_{\rm sl}(x) = \Delta U \neq \mathrm{fn}(x)$, whereas the characteristic length will be taken as the local shear layer width, *i.e.*, $\delta_{\rm sl}(x) \propto x$. Assuming constant fluid properties, *i.e.*, $\nu = \text{const.}$, this yields a local Reynolds number for shear layers that increases linearly with the streamwise coordinate, *i.e.*,

$$Re_{\rm sl}(x) \;\propto\; x \;. \tag{2a}$$

In the case of jets, the characteristic velocity will be taken as the local centerline velocity of the jet, *i.e.*, $U_{\rm j}(x) = u_{\rm c}(x) \propto x^{-1}$, while the local length scale will be taken as the local jet diameter, *i.e.*, $\delta(x) = \delta_{\rm j}(x) \propto x$, yielding a local jet Reynolds number that is a constant of the flow, *i.e.*,

$$Re_{\rm j}(x) \;\neq\; \mathrm{fn}(x) \;. \tag{2b}$$

This difference between shear layers and jets in the dependence of the local Reynolds number is interesting in the context of spatially developing flows and the evolution of the distribution of scales and turbulence spectra.

As we increase the flow Reynolds number, from small values to values approaching some minimum Reynolds number for fully-developed turbulence, the flow is able to generate ever-increasing interfacial area between the mixing species, increasing mixing and, in the case of chemically-reacting flow, chemical product formation and heat release. Beyond this transition region, *i.e.*, for $Re \gg Re_{\min}$, the Reynolds number dependence of the amount of mixed fluid can be expected to be weaker. In fact, a tenet of fully-developed turbulent flow theory is that, at high enough Reynolds numbers, the dependence of the various mean flow quantities on Reynolds number should become negligible, or vanish.

On the other hand, mixing depends on the behavior of *gradients* in the flow as well as concentration of diffusing species and the "principle of self-similarity with respect to Reynolds number cannot be expected to be applicable ..., since these gradients are determined by small-scale fluctuations." (Ref. 8, p. xvi) We will examine these propositions by comparing the outcome of experimental investigations on turbulent mixing conducted in both gas- and liquid-phase shear layers and jets.

2. Transition Reynolds numbers in shear layers and jets

A qualitative difference in the appearance of the scalar field is observed across the transition in a shear layer to a more well-mixed state, as the Reynolds number is increased, as illustrated in Fig. 1. The transition to a more well-mixed state in a gas-phase turbulent shear layer was documented by Konrad,[9] who used an aspirating probe[10] to estimate the local value of the high-speed stream fluid fraction, averaged over the resolution volume and time-response of the aspirating probe. Subsequent estimates of mixing and chemical product volume fraction in liquid-phase shear layers,[11] using a pH indicator, as well as estimates derived from probability-density functions (pdf's) measured using laser-induced fluorescence techniques,[12] documented the same behavior.

The results from the two liquid-phase shear layer measurements are plotted in Fig. 2, which depicts the estimated chemical product thickness as a function of the local Reynolds number at the measuring station. A marked increase in

FIG. 1 Laser-induced fluorescence streak images of the scalar field in a liquid-phase shear layer, for $Re \simeq 1.75 \times 10^3$ (left) and $Re \simeq 2.3 \times 10^4$ (right). Data from Ref. 12, Figs. 7 and 9, respectively.

the estimated chemical product can be seen to occur at $Re \approx 10^4$. This is also associated with a change in the pdf of the scalar fluctuations. In the pretransition region, the pdf of the conserved scalar in the flow is dominated by the near-delta-function contributions of the unmixed (pure) fluid from each of the freestreams.[12] In the posttransition regime, the composition of the mixed fluid across the layer develops a preferred value that is well-correlated with the one inferred from the estimated overall entrainment ratio for the layer.[3,12] The pdf evolves from one limit to the other in the course of this transition (*cf.* Ref. 12, Sec. 5.4, and Ref. 13), with a relatively long memory of the (typically, much larger) initial asymmetry in the relative amounts of each of the freestream fluids.

As noted in the discussions of these experiments,[11,12] finite resolution limitations in these liquid-phase experiments overestimated the absolute amount of chemical product by, roughly, a factor of two, as confirmed in chemically-reacting experiments which measured the chemical product volume fraction directly.[12] Nevertheless, the documented increase in the amount of mixing at the transition Reynolds number is qualitatively correct and was found to occur at the same Reynolds number in both gas- and liquid-phase shear layers.[14]

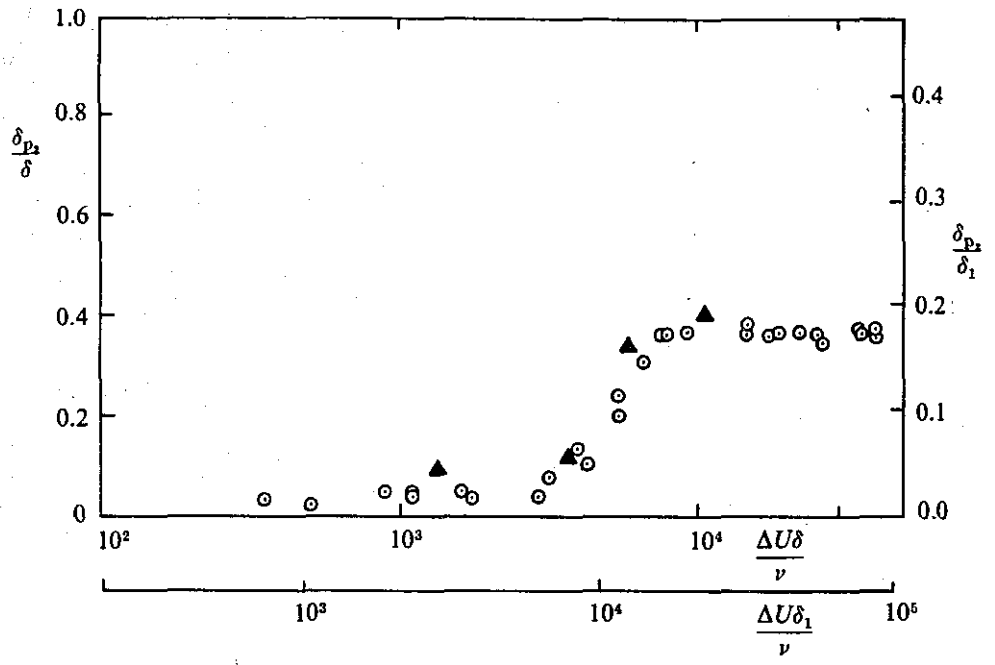

FIG. 2 Reynolds number dependence of chemical product volume fraction, in a liquid-phase shear layer, in the vicinity of the mixing transition.[12] Note that absolute values are overestimated in both experiments (see text).

The transition to a more well-mixed state, in these experiments, was correlated with the appearance of streamwise vortices and the ensuing transition to three-dimensionality of flow that is nominally two-dimensional in the initial region.[11–15] See discussion in the review paper by Roshko.[16] Corroborating evidence was also found in the numerical simulations of time-developing shear layers by Moser & Rogers that followed the developing flow to sufficiently high Reynolds numbers to document the beginning of this behavior.[17]

The transition to a more well-mixed state in turbulent jets is less conspicuous than in shear layers. Turbulent jets being three-dimensional, even at low Reynolds numbers, such a transition is not correlated with a transition to three-dimensionality in the flow field. Nevertheless, there is, again, a qualitative difference in the appearance of the scalar field for values of the Reynolds number that are lower than $Re_{\min} \approx 10^4$ and values that are comparable to that, or higher. This is illustrated in the laser-induced fluorescence images in Fig. 3, of the jet-fluid concentration in the plane of symmetry of liquid-phase jets.[18] Unmixed reservoir fluid (black) can be seen throughout the turbulent region and, in particular, all the way to the jet axis

in the lower Reynolds number (left) image at $Re_j \simeq 2.5 \times 10^3$ (imaged field spans $0 < x/d < 35$, where d is the jet nozzle diameter). This is not the case in the higher Reynolds number (right) image at $Re_j \simeq 10^4$ (imaged field spans $0 < x/d < 200$), in which jet fluid of varying concentrations can be seen to be more volume-filling within the turbulent region.

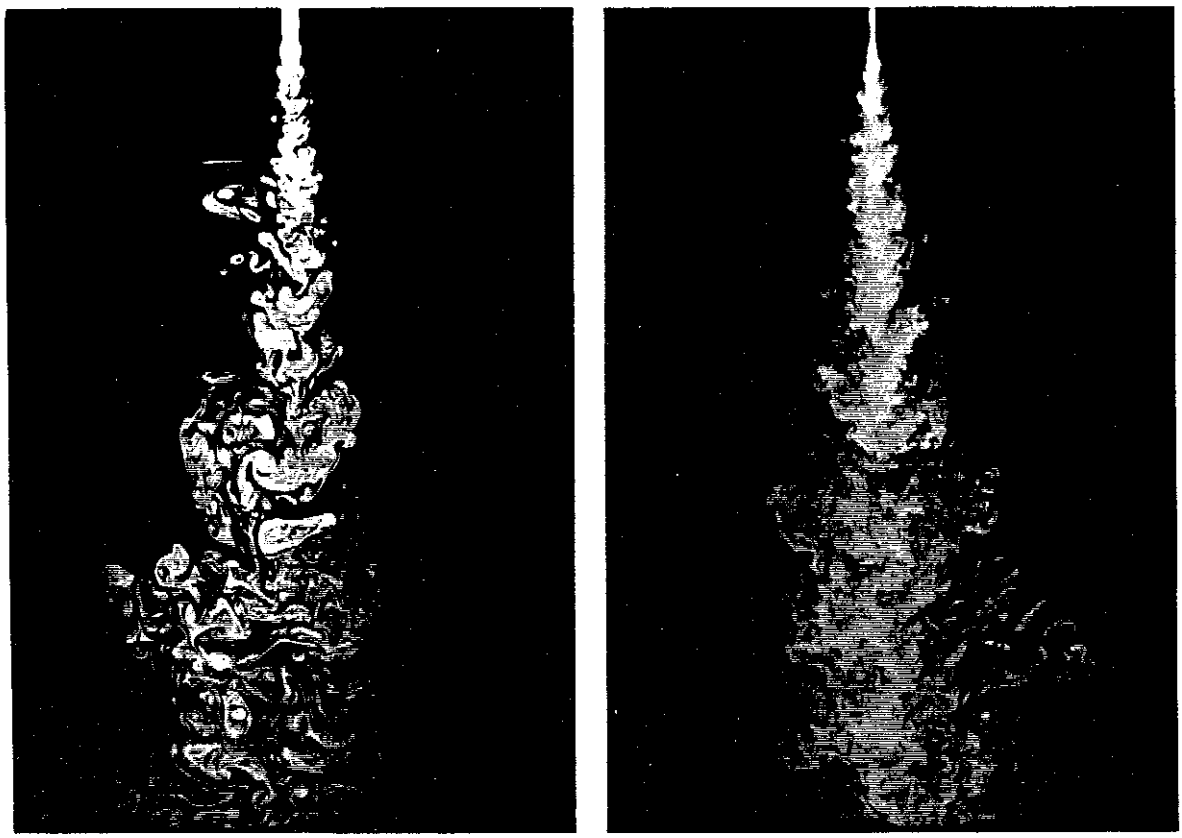

FIG. 3 Jet-fluid concentration in the plane of symmetry of a round turbulent jet. Left image: $Re_j \simeq 2.5 \times 10^3$ ($0 < x/d < 35$). Right image: $Re_j \simeq 10^4$ ($0 < x/d < 200$). Data from Ref. 18, Figs. 5 and 9.

Seitzman *et al.*[19] investigated the outer entrainment and mixing region, using laser-induced fluorescence images of OH radicals in a H_2-air turbulent diffusion flame. A qualitative evolution in the complexity of the thin burning regions can be seen, as the Reynolds number was increased from 2.3×10^3 to 4.95×10^4 (*cf.* their Fig. 3). In these experiments, this evolution is also influenced by decreasing

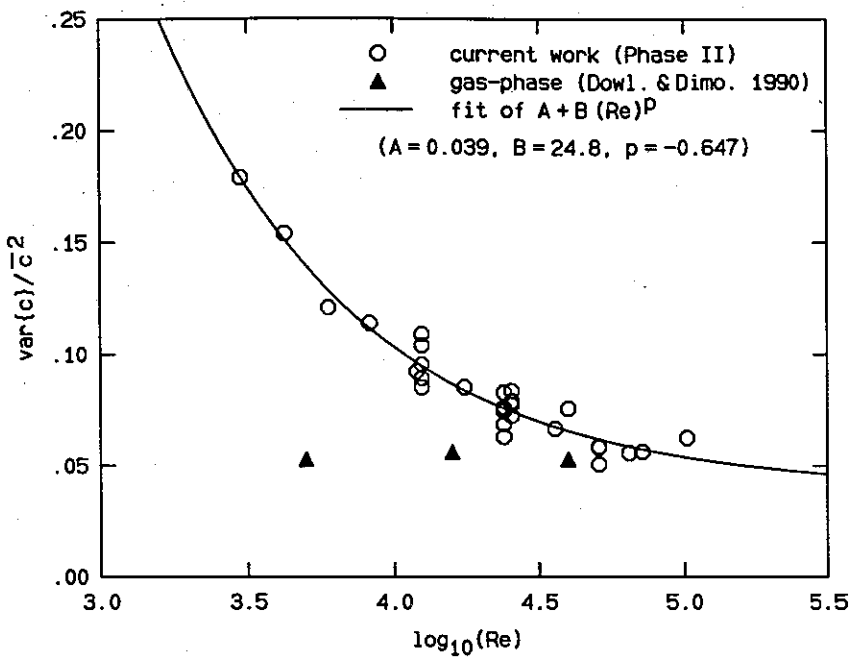

FIG. 4 Normalized variance of jet-fluid concentration on the axis of a turbulent jet, as a function of the jet Reynolds number (Ref. 22, Fig. 7.2). Circles: Liquid-phase jets.[22] Triangles: Gas-phase jets.[20]

buoyancy and the decreasing relative importance of baroclinic vorticity generation, as the Reynolds number was increased, and is, therefore, not entirely attributable to Reynolds number effects.

Similar behavior is reflected in the measurements of the rms of the scalar (jet fluid concentration) fluctuations on the axis, in the far field of gas- and liquid-phase jets, as a function of jet Reynolds number.[20–22] The data, in the form of the normalized scalar fluctuation variance, are plotted in Fig. 4 (Ref. 22, Fig. 7.2). The liquid-phase data exhibit a decrease in the fluctuation level with Reynolds number, with a rather less sensitive dependence for Reynolds numbers higher than $Re \approx 2 \times 10^4$, or so. Noting that lower fluctuation levels correspond to more homogeneous mixing, *i.e.*, a pdf of concentration values that are more tightly clustered around the local mean, we see that, at least for the case of a liquid-phase jet, the flow transitions to a more well-mixed state as the Reynolds number is increased, as in the shear layer, even though in a more gradual manner (*cf.* Fig. 2). A much weaker Reynolds number dependence of the normalized scalar variance can be seen for the gas-phase-jet data.

The Reynolds number dependence of turbulent mixing and chemical product formation in turbulent jets was recently investigated in gas-phase jets.[23,24] In this context, the turbulent diffusion flame length, L_f, is important and marks the distance from the nozzle required to mix and burn the reactant carried by the jet fluid. If the stoichiometry of the jet/reservoir reactants and jet entrainment are held constant, and for fast chemical kinetics (high Damköhler number limit), the flame length dependence on the various flow parameters provides us with a measure of the dependence of mixing on those parameters. Decreasing flame lengths, for example, imply faster (better) mixing.

The dependence of the flame length on the stoichiometry of the jet-/reservoir-fluid chemical system must first be factored in the analysis. In particular, for a momentum-dominated, turbulent jet diffusion flame, the flame length is linearly dependent on the (mass) stoichiometric mixture ratio (*e.g.*, Refs. 25–27), *i.e.*,

$$\frac{L_f}{d^*} \simeq A\,\phi_m + B \ , \tag{3}$$

where ϕ_m is the mass of reservoir fluid required to completely consume a unit mass of jet fluid. The measurements must then be regarded as investigations of the behavior of the stoichiometric coefficient, A, and normalized virtual origin (intercept), B, and their dependence, in turn, on the flow parameters.

In these experiments, long platinum wires were stretched across the turbulent diffusion flame and spaced in equal logarithmic increments along the jet axis. These permitted the line-integral of the temperature rise, $\Delta T(x,y)$, due to heat released in the chemical reaction, to be measured along the y-coordinate (transverse to the jet axis), as a function of the downstream coordinate. See Fig. 5.

The experiments utilized the $F_2 + NO$ chemical reaction, with F_2 diluted in N_2 forming the jet fluid, and NO diluted in N_2 forming the quiescent reservoir fluid. With this chemical system, an adiabatic flame temperature rise, ΔT_f, as low as 7 K was realized (with the reaction still in the fast-kinetic regime). Such low values were dictated by the results of a separate investigation that assessed the effects of buoyancy and ascertained that the measurements were realized in the momentum-dominated regime for this heat-releasing flow. The Reynolds number was varied by varying the pressure in the combustion vessel.

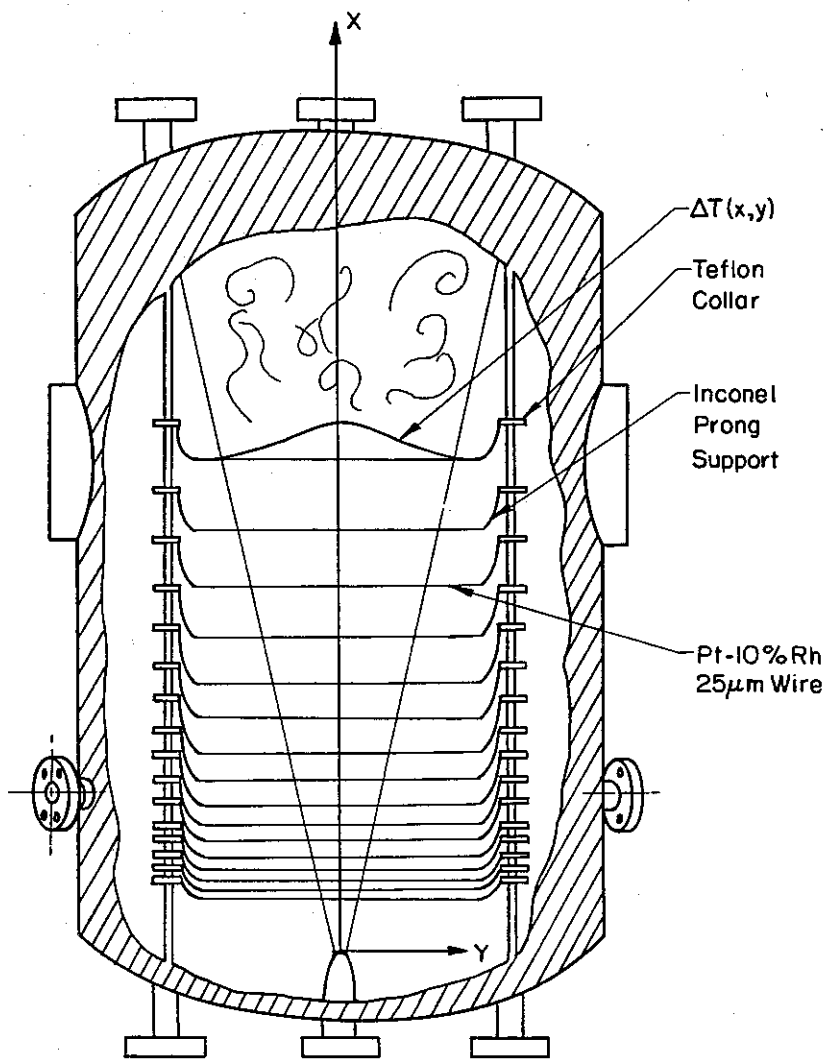

FIG. 5 Turbulent jet diffusion flame combustion vessel schematic, indicating the jet and the logarithmically-spaced temperature-sensing wire array.

If the temperature rise, $\Delta T(x,y)$, in the chemically-reacting jet is normalized by ΔT_f, the adiabatic flame temperature rise for the reaction, the line integral across the jet axis can be used to form a product thickness, $\delta_P(x)$, analogous to the one defined for shear layers, *i.e.*,

$$\delta_P(x) \equiv \int_{-\infty}^{\infty} \frac{\Delta T(x,y)}{\Delta T_f}\, dy \tag{4}$$

(*cf.* Ref. 28, Sec. 3.1.3; Ref. 29, Sec. 1.9; and Ref. 30, Eqs. 41 and discussion following). Sample data are depicted in Fig. 6, for a range of values of the (mass)

stoichiometric mixture ratio, ϕ_m. The data plot the product thickness δ_P, normalized with the length, L_w, of the platinum resistance wire used to measure the line integral, versus the logarithm of x/d^*, where d^* is the jet source diameter.[27]

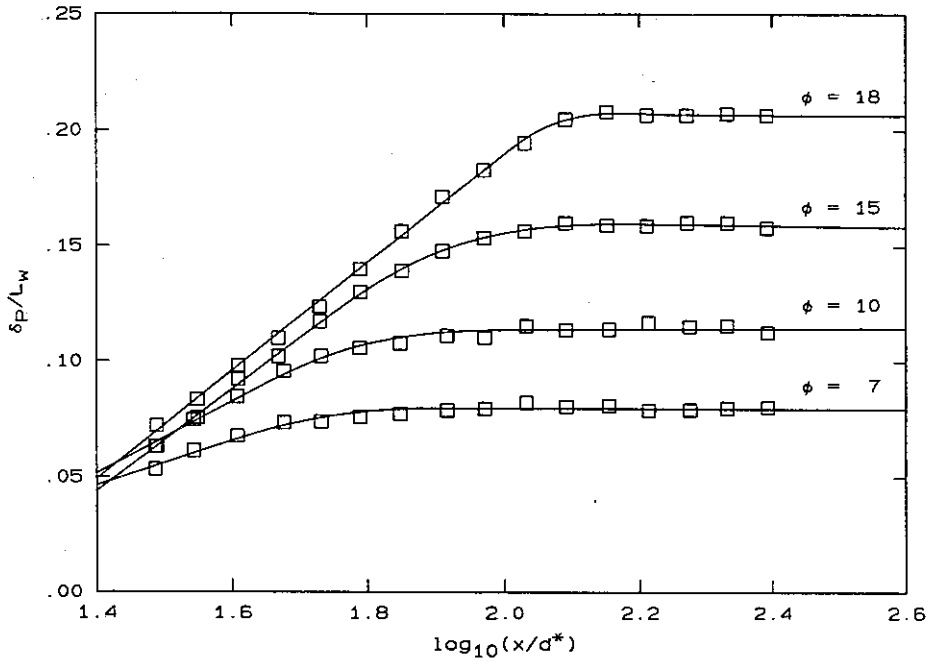

FIG. 6 Product thickness *vs.* $\log_{10}(x/d^*)$, for several stoichiometric mixture ratios (Ref. 24, Fig. 5).

To analyze these data, we note that for regions of the flow well upstream of the flame length, *i.e.*, for $x \ll L_f$, the entrained reactant is consumed on, or just outside, the boundary of the turbulent region. There, the turbulent fluid is jet-fluid-reactant rich and it need comprise only a small fraction of the mixed fluid to consume the entrained reservoir-fluid-reactant. The diffusion/reaction process then takes place in a relatively thin peripheral reaction zone at $y = \pm R_r(x)$,[a] whose ensemble-averaged radius, $R_r(x)$, is proportional to x. As a consequence, the line integral of the time-averaged temperature rise across the turbulent region increases as the chemical reaction releases heat in the thin reaction zones at the edges of the turbulent region.

[a] This picture is corroborated by the OH-images obtained by a number of investigators in H_2-air jet flames (*cf.* Refs. 19 and 31, for example).

It was conjectured that the radial integral of the temperature rise, at a given station x, increases in proportion to the entrainment velocity at that station, $u_e[R_r(x)]$, *i.e.*,

$$\frac{\mathrm{d}}{\mathrm{d}x}\int_0^\infty \Delta T(x,r)\,\mathrm{d}r \;\propto\; u_e[R_r(x)]\,\Delta T_f \;, \tag{5}$$

or, for a momentum-driven, turbulent jet,

$$\mathrm{d}\int_{-\infty}^{\infty}\frac{\Delta T(x,y)}{\Delta T_f}\,\mathrm{d}y \;\propto\; \frac{\mathrm{d}x}{2\pi R_r(x)} \;\propto\; \frac{\mathrm{d}x}{x} \;. \tag{6}$$

Integrating this relation and scaling with the flame length L_f, we have

$$\frac{\delta_P(x \ll L_f)}{L_f} \;\simeq\; a\,\log\left(\frac{x}{L_f}\right) + b \;. \tag{7}$$

This dependence of the line integral on x suggested the logarithmic wire spacing used in the experiment and was used in the analytical form of the fit for the line-integrated, time-averaged, temperature-rise data (*cf.* Fig. 6).

Beyond the end of the flame region, *i.e.*, for $x > L_f$, no further heat is released and, in the absence of buoyancy effects, the temperature excess becomes a passively-convected scalar with a self-similar profile. In that case,

$$\Delta T(x,y) \;\simeq\; \Delta T(x,0)\,f\left(\frac{y}{x}\right) \;\propto\; \frac{1}{x}\,f\left(\frac{y}{x}\right)$$

and the product thickness line integral becomes independent of the downstream coordinate, x, *i.e.*,

$$\delta_P(x > L_f) \;\propto\; \int_{-\infty}^{\infty}\frac{1}{x}\,f\left(\frac{y}{x}\right)\,\mathrm{d}y \;\neq\; \mathrm{fn}(x) \;. \tag{8}$$

As can be seen in Fig. 6, the experimental results confirmed the conjecture for $x \ll L_f$. They were also consistent with the anticipated conserved-scalar behavior of the temperature rise for $x > L_f$, *i.e.*, a product thickness that asymptotes to a constant value. Such data allow us to estimate the flame length, L_f. In particular, one can accept an operational definition of L_f as the location where the product thickness line integral (Eq. 4) has attained 99% of its asymptotic value, as one does on the basis of a boundary layer velocity profile, for example.

Figure 7 (Ref. 23, Fig. 4.8) plots the stoichiometric coefficient, A, in the expression for the flame length (*cf.* Eq. 3), *i.e.*, the slope of the flame length *vs.* the stoichiometric mixture ratio ϕ_{m}. This can be regarded as the additional length, in units of the jet source diameter d^*, required to entrain, mix, and react with a unit increase in the stoichiometric ratio of the jet-/reservoir-fluid chemical system, *i.e.*,

$$A \equiv \frac{\mathrm{d}}{\mathrm{d}\phi_{\mathrm{m}}} \left(\frac{L_{\mathrm{f}}}{d^*} \right) . \tag{9}$$

In the fast kinetic regime, as was the case in these experiments, this quantity is a useful measure of mixing. It separates the self-similar, far-field behavior from that of the virtual origin in the overall mixing process.

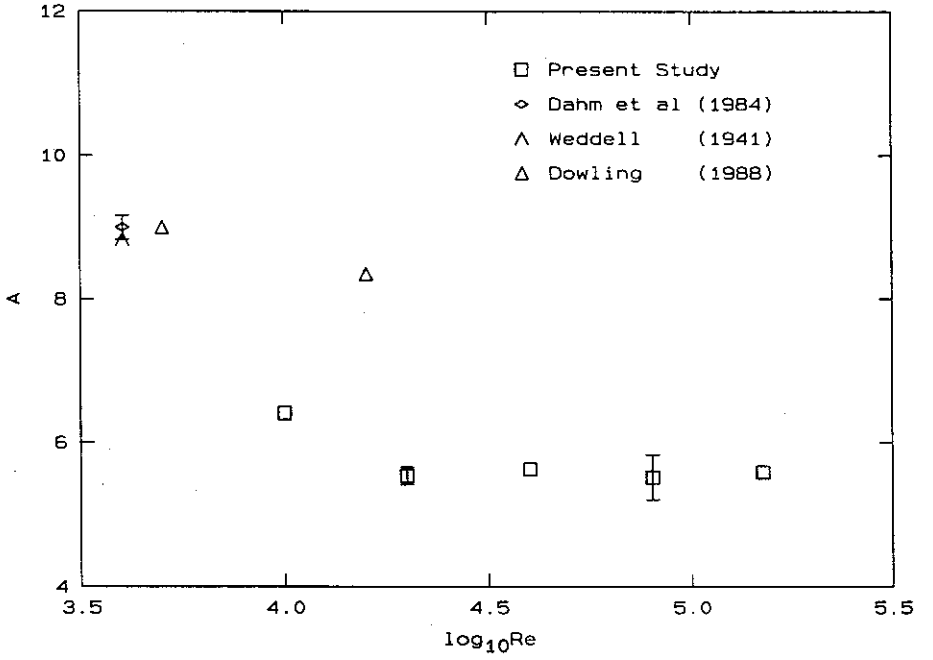

FIG. 7 Flame length stoichiometric coefficient A (Eq. 3). Squares: Gas-phase chemically-reacting jet data.[23] Diamond: Laser-induced fluorescence, liquid-phase data.[32] Lambda: pH-indicator, liquid-phase data.[25,33] Triangles: Flame length data inferred from gas-phase, nonreacting data (see text).[34]

The data in Fig. 7 indicate that mixing in the far field of a turbulent jet improves relatively rapidly with increasing Reynolds number. Specifically, A decreases until a Reynolds number of, roughly, 2×10^4, with a much weaker dependence on Reynolds

number, if any, beyond that. These data are in accord with the nonreacting, liquid-phase data in Fig. 4, which also indicate improved mixing up to Reynolds numbers of 2×10^4, or so, with a weaker dependence beyond that. The latter data, however, do not permit the separation of the far-field and virtual-origin contributions to the overall mixing process, as do the chemically reacting jet data. We should also note that the near- and intermediate-field behavior, which contributes to the virtual origin of the mixing process and the resulting flame length, does not exhibit the same Reynolds number dependence.[23]

A potential difficulty should be recognized between the inferred behavior based on the nonreacting, gas-phase jet data (triangles),[34] and the chemically-reacting, gas-phase data (squares).[23] Two observations are relevant here. The values estimated from the nonreacting gas-phase data (triangles) were derived assuming certain similarity properties of the concentration pdf and the virtual origin of the whole process (see discussion in Ref. 34, Sec. 5.4, and Ref. 21, Appendix B).

Partly as a consequence, as was also noted in the comparison between the data in Figs. 4 and 7, it is not possible to separate the contribution to the flame length of the (rather large) virtual origin of the mixing process, and its dependence on Reynolds number,[23] from the Reynolds number dependence of the far-field mixing process, *i.e.*, the dependence of the flame length stoichiometric coefficient, A.

While this may be a minor point, we may wish to note that transition Reynolds numbers for jets seem to be twice as large as for shear layers. On the one hand, the two flows are sufficiently different to admit differences in their behavior of a factor of 2, or so, in Reynolds number. On the other, however, if the characteristic large scale $\delta(x)$ chosen for the local Reynolds number definition of a jet is the local *radius*, as would be appropriate if the length scale in the general case is defined as the transverse spatial extent across which the shear is sustained, then the transition Reynolds number for jets becomes very close to that for shear layers.

3. Mixing in fully-developed turbulence

In fully-developed turbulent shear layers, beyond the mixing transition, mixing also exhibits a weaker dependence on Reynolds number. Figures 8a and 8b plot experimentally obtained data of the normalized chemical product thickness, *i.e.*,

$$\frac{\delta_P(x;\phi)}{\delta(x)} = \frac{1}{\delta(x)} \int_{-\infty}^{\infty} \frac{\Delta T(x,y;\phi)}{\Delta T_f(\phi)}\, dy \tag{10}$$

(*cf.* Eq. 4), for both low (Fig. 8a) and high (Fig. 8b) values of the stoichiometric mixture ratio ϕ. The stoichiometric mixture ratio, in this case, denotes the parts (moles) of high-speed fluid required to consume a part (mole) of low-speed fluid in the shear layer mixing zone (*e.g.*, Ref. 30). The product thickness data in Figs. 8a and 8b were normalized by the 1% temperature rise product thickness, δ_T, which has been found to be close to the visual thickness, δ_{vis}, of the shear layer.[1,12,30,35]

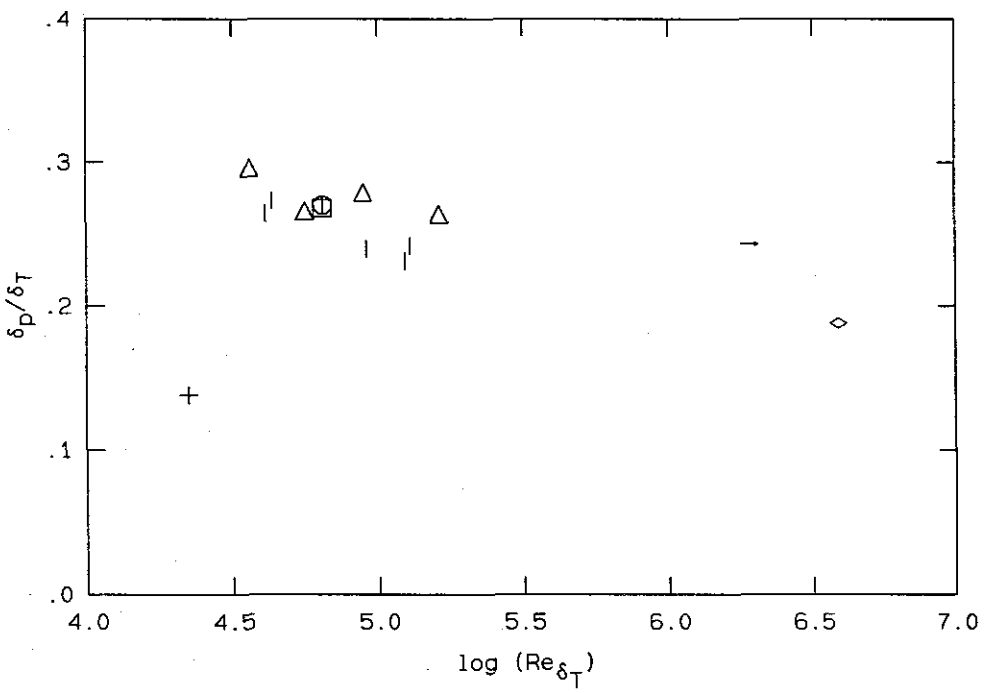

FIG. 8a Low-ϕ normalized product thickness *vs.* Reynolds number for a turbulent shear layer. Matched free-stream density, incompressible, gas-phase shear layers: $\phi = 1/8$ (square), $\phi = 1/4$ (circle).[35] Vertical lines: $\phi = 1/8$.[36] Triangles: $\phi = 1/8$.[37] Supersonic shear layers: $\phi = 1/4$, $\rho_2/\rho_1 = 0.71$, $M_c = 0.51$ (arrow); $\phi = 1/3$, $\rho_2/\rho_1 = 5.95$, $M_c = 0.96$ (diamond).[38] Liquid-phase shear layer: $\phi = 1/10$ (cross).[12]

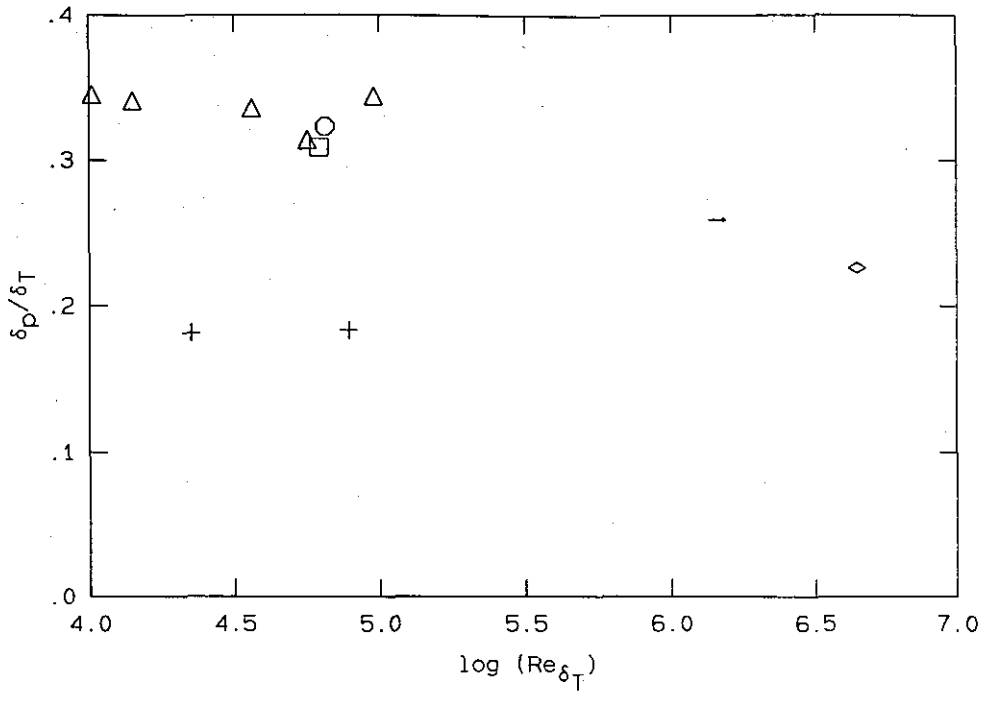

FIG. 8b High-ϕ shear layer normalized product thickness *vs.* Reynolds number. Matched free-stream density, incompressible, gas-phase shear layers: $\phi = 8$ (square), $\phi = 4$ (circle).[35] Triangles: $\phi = 8$.[37] Supersonic shear layers: $\phi = 4$, $\rho_2/\rho_1 = 0.71$, $M_c = 0.51$ (arrow); $\phi = 3$, $\rho_2/\rho_1 = 5.95$, $M_c = 0.96$ (diamond).[38] Liquid-phase shear layer: $\phi = 10$ (crosses).[12]

These data were all derived from chemically-reacting shear layer experiments, conducted in the fast chemical-kinetic regime, *i.e.*, high Damköhler number limit. In this limit, all molecularly mixed fluid produces chemical product, as dictated by the stoichiometry of the mixed fluid composition (*cf.* discussion in Ref. 30, Sec. IV).

The chemically reacting experiments were conducted for low and high values of the (molar) stoichiometric mixture ratio, ϕ, that can be expected to yield near-stationary values of the product thickness $\delta_P(\phi)$, with respect to ϕ. The chemical product thickness has a rather sensitive dependence on ϕ, as the stoichiometric mixture fraction, $\xi_\phi = \phi/(\phi+1)$, approaches zero or unity, as a result of the regions near the delta functions corresponding to the pure fluid in the composition pdf.[39,40] Data points indicated by crosses were derived from experiments in liquid-phase flows.[12] All other data were based on results from gas-phase flows. The plotted points based on the experiments by Frieler[37] and Hall *et al.*[38] were calculated by

Chris Bond from the original temperature-rise data.[b] Data at the highest values of the Reynolds number were derived from chemically-reacting, supersonic shear layers ($M_1 > 1$, $M_2 < 1$)[38] and, as a consequence, can be assumed to be susceptible to the combined effects of compressibility as well as Reynolds number. We note here that even though the velocity ratio, $r \equiv U_2/U_1$, for the supersonic shear layer experiments was very low, and should perhaps not be included in the same plot as the subsonic shear layer experiments for which $r \simeq 0.4$, the *molar* entrainment ratio, E_n, *i.e.*, the ratio of the number of high-speed freestream fluid moles per mole of low-speed freestream fluid entrained, was estimated to be close to its value for the incompressible flow experiments. Specifically, for the incompressible flow experiments,[3,12,35] $E_n \simeq 1.3$. The estimated values for the compressible shear layers were $E_n \simeq 1.07$, for the $M_c \simeq 0.51$ shear layer ($r \simeq 0.24$), and $E_n \simeq 1.2$, for the $M_c \simeq 0.96$ shear layer ($r \simeq 0.10$).[38,41,42]

Several observations can be made on the basis of these data:

a. In the limit of fast kinetics, the chemical product formed decreases as the Reynolds number increases. This implies less efficient mixing in fully-developed shear layers as the Reynolds number increases. Presently available data suggest that this is opposite the behavior exhibited by turbulent jets (recall data in Figs. 4 and 7, and related discussion).

b. The data admit a Reynolds number dependence of the chemical product thickness for the low-ϕ case (Fig. 8a) that is stronger than the high-ϕ case (Fig. 8a).[c] If this is proven to be the case, it would imply a complicated dependence of the pdf of compositions on Reynolds number.

c. Liquid-phase shear layer mixing exhibits a weaker Reynolds number dependence than gas-phase shear layer mixing (*cf.* Fig. 8b). Unless the data for turbulent jets should all be regarded as not in fully-developed flow (*cf.* Fig. 4), this is also opposite the behavior found in turbulent jets.

---

[b] Private communication.

[c] Recall that, for these flows, the high-speed stream fluid is preferentially entrained.[3]

Based on the presently available scant experimental data and unless the region $2 \times 10^5 < Re < 10^6$ conceals a second transition to a Reynolds-number-independent turbulent mixing state,

d. the trend in Figs. 8a and 8b suggests that, at least at low compressibility, *e.g.*, up to the lower of the two convective Mach numbers investigated, Reynolds number effects dominate compressibility effects.

The latter observation must be regarded as the most tentative and must await the results of further experimental investigations to be confirmed.

It is interesting that in the case of mixing in turbulent jets, gas-phase data for the flame length indicate only a weak Reynolds number dependence beyond the mixing transition, if any (Fig. 7). Measurements in liquid-phase jets, however, at Reynolds numbers as high as 7.2×10^4, yield scalar spectra that have not converged to a Reynolds-number-independent state,[43] in accord with the data in Fig. 4.

Finally, it is noted that some of these observations are at variance with the inferences drawn in a review by Broadwell & Mungal,[44] of earlier data. The interested reader is directed to that discussion for further details.

4. Transition Reynolds numbers in other flows

The observations of mixing transitions in shear layers and jets suggest that a minimum Reynolds number may be required for turbulence to develop into a more well-mixed state in these flows. Specifically, we must have $Re > Re_{\min}$, with $Re_{\min}$ in the neighborhood of 0.5×10^4 to 2×10^4, for fully-developed turbulent flow. It is interesting that this value does not appear to be peculiar to the far-field behavior in turbulent jets and free-shear layers. Other flows also exhibit similar transitions at comparable values of the Reynolds number, as we'll discuss below.

Pipe flow, for example, transitions out of its slug/puff regime to a less intermittent, fully-turbulent state over a range of Reynolds numbers that depend on the entrance conditions. This sensitivity to initial conditions diminishes, however, at a Reynolds number in the vicinity of 10^4 .[45]

The Coles' turbulent boundary layer wake parameter, Π, that scales the outer flow region of a turbulent boundary layer,[46] is found to increase with Reynolds number, for a zero-pressure-gradient boundary layer, attaining an asymptotic value of $\Pi = 0.620$ at a Reynolds number, based on displacement thickness,[47] of $Re \equiv U_\infty \delta^* / \nu \simeq 0.8 \times 10^4$. See Refs. 48 and 49, for a discussion, and Ref. 49, Table 4 and Fig. 6, for a compilation of low-speed, turbulent boundary-layer flow data.

In experiments by Liepmann & Gharib, in the near field of turbulent jets, the number of azimuthal nodes in vortex structures becomes difficult to identify beyond a certain Reynolds number, where the flow transitions to a much more chaotic state.[50] The authors correlate this transition with a laminar-turbulent transition in the jet nozzle boundary layers. It is also interesting, however, that it occurs at a Reynolds number very close to 10^4.

In recent experiments on lifted-flame behavior, Hammer notes a change in the scaled lift-off height of turbulent jet flames at a jet Reynolds number, in the neighborhood of $Re \approx 1.8 \times 10^4$, beyond which the Reynolds number dependence is weaker. See data in Ref. 51, Fig. 3.8, and discussion following.

In his review of bluff-body flows, Roshko documents several regimes, as indicated by the behavior of the base pressure of a circular cylinder, as a function of Reynolds number.[52] In particular, the (negative) base pressure is found to increase in the range of Reynolds numbers of $0.3 \times 10^4 < Re \equiv U_\infty d_{\rm cyl} / \nu < 2 \times 10^4$ (Ref. 52, Fig. 1). Roshko attributes this behavior to a transition in the separating shear layers.

Measurements of the scaled turbulent kinetic energy dissipation rate,

$$\alpha = \frac{\varepsilon \ell}{u'^3} , \tag{11}$$

in flow behind square grids, where ε is the kinetic energy dissipation per unit mass, ℓ is the longitudinal length scale, and u' is the rms streamwise velocity fluctuation level, suggest that it decreases relatively rapidly with increasing Taylor Reynolds number,

$$Re_{\rm T} \equiv \frac{u' \lambda_{\rm T}}{\nu} , \tag{12a}$$

where λ_T is the Taylor microscale, until a value of $Re_T \approx 70$, and then becomes much less sensitive to Reynolds number, attaining a value of $\alpha \approx 1$ at higher Reynolds numbers. This value may not be universal, however, with measured values in the range $1 < \alpha < 2.7$ behind non-square grids.[53]

A similar conclusion was arrived at by Jimenez *et al.*,[54] in their numerical simulations of turbulence in a spatially-periodic cube, in the range $36 < Re_T \leq 170$. They report a value of $\alpha \simeq 0.65$ attained for $Re_T \geq 95$. Since

$$Re_T \approx Re^{1/2} , \tag{12b}$$

it, again, appears that $Re > Re_{min} \approx 10^4$ is a necessary condition for fully-developed turbulent flow.[55]

In thermal convection, a transition from "soft turbulence" to "hard turbulence" has been noted for Rayleigh numbers given by $Ra \approx 10^8$, that is marked by a qualitative change in the pdf of the measured temperature fluctuations.[56] Since $Re \approx Ra^{1/2}$ for this flow,[57] we again recover a minimum Reynolds number boundary of the fully-developed turbulent state at $Re \approx 10^4$.

Careful experiments were recently performed that measured the torque in Couette-Taylor flow, in the range of Reynolds numbers of $800 < Re < 1.23 \times 10^6$.[58,59] These experiments revealed a "well-defined, non-hysteretic transition" in a narrow range of Reynolds numbers, $10^4 < Re_{tr} < 1.3 \times 10^4$. The flow was found to be qualitatively different, below and above this transition, as illustrated in the flow-visualization data reproduced in Fig. 9, with pre- and post-transition differences reminiscent of the corresponding ones in jets (*cf.* Fig. 3). See also additional flow-visualization data in Ref. 58, Figs. 1a,b. Beyond this transition, the dependence of the torque on Reynolds number becomes progressively weaker. Significantly, however, the torque does not attain viscosity-independent behavior to the highest Reynolds numbers investigated.

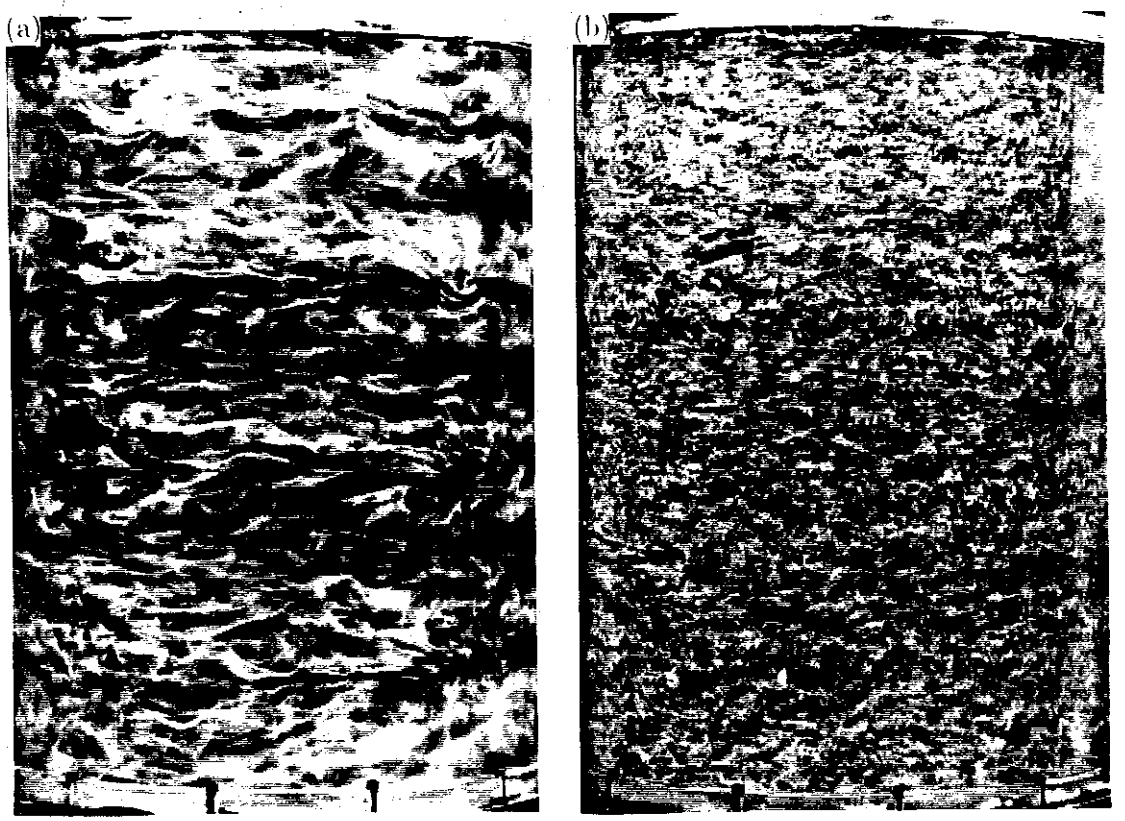

FIG. 9 Couette-Taylor flow-visualization data at (a) $Re = 0.6 \times 10^4$, and (b) $Re = 2.4 \times 10^4$. From Ref. 59, Figs. 5a,b, reproduced by kind permission of Prof. H. Swinney.

5. A criterion for fully-developed turbulence?

The preceding observations suggest there may exist a property of turbulence that induces it to transition to a more well-mixed state, is associated with Reynolds numbers in excess of $Re_{\min} \approx 10^4$, and appears to be rather independent of the details of the flow geometry. The following is a proposed ansatz to account for this behavior.

That this transition appears to be independent of the flow geometry indicates that the explanation should not be sought in the large-scale dynamics, or the development of distinct features and organized patterns in these flows. These are, typically, flow-geometry dependent. One is rather led to consider the physical significance of the various scales of turbulence and their Reynolds number scaling.

The 1941 Kolmogorov proposals hypothesize that the dynamics in the (inertial) range of scales λ that are unaffected by the outer scale δ, but are large compared to the inner, dissipation (Kolmogorov) scale,

$$\lambda_K \equiv \left(\frac{\nu^3}{\varepsilon}\right)^{1/4} , \tag{13}$$

i.e., for

$$\lambda_K \ll \lambda \ll \delta , \tag{14}$$

can be treated in a universal, self-similar fashion. In this range of scales, for example, the energy spectrum is predicted (and found) to exhibit a power-law behavior with a $-5/3$ exponent.[60]

To refine the bounds in Eq. 14, we appreciate that independence from the dynamics of the outer scale, δ, requires that the scale λ be smaller than a scale that can be generated directly from the outer scale δ. Such a scale would an outer laminar layer thickness, λ_L, that can be generated by a single δ-size sweep across the whole transverse extent of the turbulent region, for example. The size of this scale can be estimated in terms of the 99% thickness of a Blasius boundary layer, for example, that is growing over a spatial extent δ, *i.e.*,

$$\frac{\lambda_L}{\delta} \simeq 5.0\, Re^{-1/2} . \tag{15}$$

It is a scale connected by viscosity to the outer scale, δ, of the flow. By virtue of its dependence on Reynolds number (*cf.* Eqs. 12 and 15), this scale, as noted by H. W. Liepmann in private conversation many years ago, is closely related to the Taylor microscale, λ_T.

At the other end of the spectrum, the requirement that the motions must be inviscid with respect to the inner dissipation scales dictates that the local scale λ must be large with respect to an inner viscous scale, λ_ν (*cf.* Fig. 10) that can be taken as proportional to the (defined) Kolmogorov dissipation scale, λ_K. This allows us to refine the inequality that bounds the inertial range of scales (Eq. 14) to the one below, *i.e.*,

$$\frac{\lambda_K}{\delta} < \frac{\lambda_\nu}{\delta} \ll \frac{\lambda}{\delta} \ll \frac{\lambda_L}{\delta} < 1 , \tag{16}$$

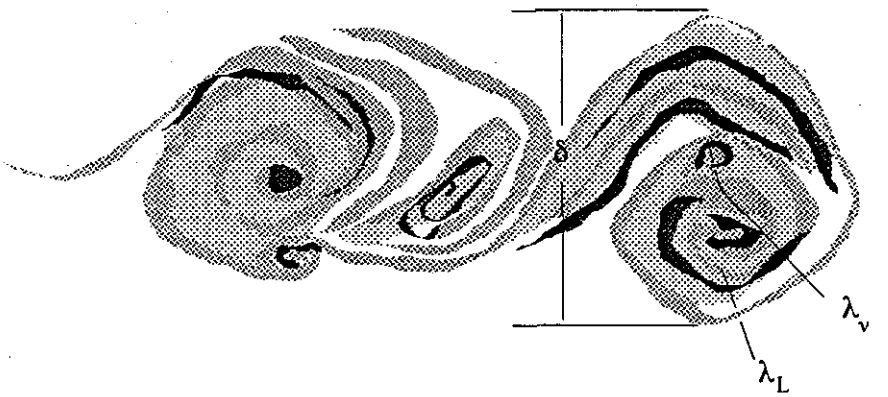

FIG. 10 Schematic of the outer scale, δ; the Taylor scale, λ_T; and the viscous scale, λ_ν, in a sheared turbulent region.

as a necessary condition for fully-developed flow.

To translate this inequality to a relation for the Reynolds number, we need the Reynolds number dependence of the ratio of the various scales to the outer scale δ. We can rely on Eq. 15 for the estimate of the outer laminar-layer thickness, λ_L, suggested by Liepmann. Following on his suggestion, it is interesting to compare that to the Taylor scale for a turbulent jet, for example. For turbulence in the far field of a jet, the Taylor scale, λ_T, can be estimated from the Taylor Reynolds number on the jet axis (Eq. 12). This is approximately given by

$$Re_T \simeq 1.4\, Re^{1/2} , \tag{17}$$

on the jet axis.[20,21] Using the value of $u' \simeq 0.25\, u_c$, on the axis of the turbulent jet, and $\delta(x) \simeq 0.4\,(x - x_0)$ for the local jet diameter, we obtain

$$\frac{\lambda_T}{\delta} \simeq 2.3\, Re^{-1/2} , \tag{18}$$

which is a little smaller but close to the Liepmann laminar-layer thickness, λ_L (a prefactor of 2.3 for λ_T, *vs.* 5.0, for λ_L), especially considering that it is estimated from flow properties on the jet axis.

An appropriate inner viscous scale, λ_ν, can be estimated in terms of the wave-number k_ν, where the energy spectrum deviates from the $-5/3$ power-law behavior, or, $k_\nu \lambda_K \simeq 1/8$.[61,62] This yields,[63]

$$\lambda_\nu \approx \frac{2\pi}{k_\nu} \simeq 50\, \lambda_K . \tag{19}$$

To estimate the Reynolds number and outer scale dependence of λ_ν, we can use the expression from Friehe *et al.*,[20,64] for the energy-dissipation rate on the jet axis, in the far field, *i.e.*,

$$\varepsilon \simeq 48 \frac{u_0^3}{d_0} \left(\frac{d_0}{x - x_0} \right)^4 , \tag{20}$$

where u_0 is the jet nozzle velocity, d_0 is the jet nozzle diameter, and x_0 is the virtual origin of the far field turbulent flow. Substituting in Eq. 13 we then have

$$\frac{\lambda_K}{\delta} \simeq 0.95\, Re^{-3/4} , \tag{21}$$

and, therefore, for a turbulent jet,

$$\frac{\lambda_\nu}{\delta} \simeq 50\, Re^{-3/4} . \tag{22}$$

Substituting for λ_L, λ_ν, and λ_K in Eq. 16, we obtain

$$Re^{-3/4} < \frac{\lambda_{min}}{\delta} \approx 50\, Re^{-3/4} \ll \frac{\lambda}{\delta} \ll \frac{\lambda_{max}}{\delta} \approx 5.0\, Re^{-1/2} < 1 . \tag{23}$$

The range of intermediate inviscid scales, *i.e.*, scales smaller than λ_L but larger than λ_ν, can be seen to grow rather slowly with Reynolds number. Specifically, the ratio

$$\mathcal{N} = \frac{\lambda_{max}}{\lambda_{min}} , \tag{24a}$$

which measures the extent of the uncoupled range of spatial scales, *i.e.*, the number of viscous scales within a Taylor scale, is given by

$$\mathcal{N} \approx 0.1\, Re^{1/4} , \tag{24b}$$

where the (approximate) factor of 0.1 was estimated for a turbulent jet. This is indicated schematically in Fig. 11. In other flows, we can expect the uncoupled range of scales to exhibit the same Reynolds number dependence (Eqs. 24a,b), with, possibly, a different prefactor, however.

On the basis of these observations, it can be argued that a necessary condition for fully-developed turbulence and the 1941 Kolmogorov similarity ideas to apply is the existence of a range of scales that are uncoupled from the large scales, on the one hand, and are free from the effects of viscosity, on the other. Considering that we must have

$$\frac{\lambda_L}{\lambda_\nu} \simeq \frac{\lambda_{max}}{\lambda_{min}} = \mathcal{N} > 1 , \tag{24c}$$

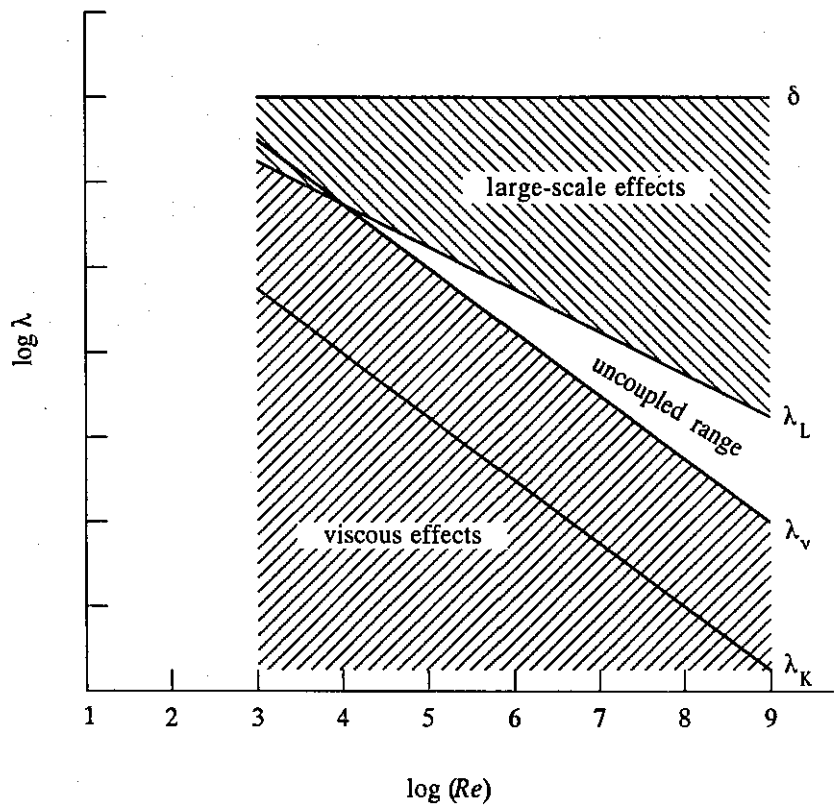

FIG. 11 Reynolds number dependence of spatial scales for a turbulent jet.

with some margin, we see that the existence of such a range of scales requires a minimum Reynolds number of the order of 10^4 (Eq. 24b); a value in accord with the minimum Reynolds number identified for transition to fully-developed, well-mixed turbulent flows.

Jimenez *et al.* performed measurements of velocity fluctuations in a two-dimensional shear layer and found a power-law regime in the energy spectrum, with an exponent close to $-5/3$, developing in the neighborhood of the mixing transition.[65] Subsequent investigations of the mixing transition by Huang and Ho also associated the development of a $-5/3$ spectral regime with the mixing transition, correlating it, however, with the number of pairings rather than with local values of the Reynolds number.[66] Nevertheless, in both these investigations, the Reynolds number in the vicinity of the mixing transition and the development of the $-5/3$ spectrum regime was found to be in the range of $3 \times 10^3 < Re(x) < 10^4$, in accord with the range documented in Fig. 2. To the extent that the appearance of a $-5/3$ spectral regime marks the development of an inertial range of scales and the applicability of the

1941 Kolmogorov ideas, these experiments lend further credence to the ansatz.

6. Conclusions

The preceding discussion of the experimental evidence and the theoretical ansatz supports the notion that fully-developed turbulence requires a minimum Reynolds number of the order of 10^4 to be sustained. This value must be viewed as a necessary, but not sufficient, condition for the flow to be fully-developed. Presently available evidence suggests that both the fact that the phenomenon occurs and the range of values of the Reynolds number where it occurs are universal, *i.e.*, independent of the flow geometry.

On the other hand, how sharp this transition is *does* appear to depend on the details of the flow. In particular, it is remarkably sharp, as a function of Reynolds number, in the (Couette-Taylor) flow between concentric rotating cylinders. It is less well-defined for a shear layer and, among the flows considered, the least well-defined for turbulent jets. Perhaps an explanation for this variation lies in the definition of the Reynolds number itself (Eq. 1) and the manner in which the various factors that enter are specified for each flow. In the case of the Couette-Taylor flow, for example, both the velocity $U_{\rm CT} = \Omega\, a$ and the spatial scale $\delta_{\rm CT} = b - a$, where Ω is the differential rotation rate, with a and b the inner and outer cylinder radii, are well-defined by the flow-boundary conditions.[59]

In the case of a zero streamwise pressure-gradient shear layer, the velocity $U_{\rm sl} = \Delta U = U_1 - U_2$ is a constant, reasonably well specified by the flow boundary conditions at a particular station. The length scale $\delta_{\rm sl} = \delta_{\rm sl}(x) = \langle\, \delta(x,t) \,\rangle_t$, however, must be regarded as a stochastic variable in a given flow with a relatively large variance. The Reynolds number for the shear layer is then the product of a well-defined variable and a less well-defined, stochastic variable.

In the case of a turbulent jet, both the local velocity $U_{\rm j} = U_{\rm j}(x) = \langle\, u_{\rm c}(x,t) \,\rangle_t$ and the length scale $\delta_{\rm j} = \delta_{\rm j}(x) = \langle\, \delta_{\rm j}(x,t) \,\rangle_t$, or $\delta_{\rm j}(x) = \langle\, R(x,t) \,\rangle_t$, the local jet radius, must be regarded as stochastic flow variables, each with its own large variance. The Reynolds number for the jet is then the product of two stochastic

variables and, as a consequence, its local, instantaneous value is the least well-defined of the three.

Viewing the Reynolds number itself as a stochastic variable, it would appear that the hierarchy of the sharpness of the transition to the fully-developed turbulent state is correlated with the sharpness with which the flow and the boundary conditions allow the values of the local Reynolds number to be specified to the dynamics.

A related issue also arises as a consequence of the definition of the local Reynolds number. As noted in the discussion of Eqs. 1 and 2, the Reynolds number for a shear layer increases with the downstream coordinate, whereas the Reynolds number for a jet is a constant of the flow. As a consequence, a shear layer may possess regions with local Reynolds numbers below the minimum and transition to fully-developed turbulence, *within the spatial extent of the same flow*, if its streamwise extent is large enough. A turbulent jet, on the other hand, is either fully developed over its whole extent, or is not. This is also relevant to the description and dynamics in other flows.

As regards fully-developed turbulent flow, the presently available evidence does not support the notion of Reynolds-number-independent mixing dynamics, at least in the case of gas-phase shear layers for which the investigations span a large enough range. In the case of gas-phase turbulent jets, presently available evidence admits a flame length stoichiometric coefficient A (*cf.* Eq. 3) tending to a Reynolds-number-independent behavior (*cf.* Fig. 7). We appreciate, however, that the range of Reynolds numbers spanned by experiments to date may not be large enough to provide us with a definitive statement, at least as evidenced by the range required in the case of shear layers (*cf.* Figs. 8). Secondly, the flame-length virtual origin, B (Eq. 3), possesses a maximum in the neighborhood of the transition Reynolds number of $Re \approx 2 \times 10^4$ and does not appear to attain a Reynolds-number-independent behavior in the same range of Reynolds numbers.[23] We should also recall that the torque in Couette-Taylor flow does not attain a Reynolds-number-independent behavior to the highest values of the Reynolds number investigated.[59] Neither, of course, does the skin-friction coefficient in a turbulent boundary layer over a smooth

flat plate.

In comparing shear-layer with turbulent-jet mixing behavior, the more important conclusion may be that they appear to respond in the opposite way to Schmidt number effects, *i.e.*, gas- *vs.* liquid-phase behavior. Specifically, it is high-Schmidt number (liquid-phase) shear layers that exhibit a low Reynolds-number dependence in chemical product formation, if any (*cf.* Fig. 8b). In contrast, it is gas-phase turbulent jets that exhibit an almost Reynolds-number-independent normalized variance of the jet-fluid concentration on the jet axis, with a strong Reynolds-number dependence found in liquid-phase jets, in the same Reynolds-unber range (*cf.* Fig. 4).

To summarize, recent data on turbulent mixing, as well as evidence garnered in other contexts, support the notion that fully-developed turbulent flow requires a minimum Reynolds number of 10^4, or a Taylor Reynolds number of $Re_T \approx 10^2$, to be sustained. Conversely, turbulent flow below this Reynolds number cannot be regarded as fully-developed and can be expected to be qualitatively different.

The manifestation of the transition to this state may depend on the particular flow geometry, *e.g.*, the appearance of streamwise vortices and three-dimensionality in shear layers. Nevertheless, the fact that such a transition occurs, as well as the approximate Reynolds number where it is expected, appears to be a universal property of turbulence. It is observed in a wide variety of flows and turbulent flow phenomena.

In contrast, studies of mixing in fully-developed turbulent jets and shear layers suggest that we cannot hope for a universal description of turbulent mixing. The dimensionless parameters that scale the relative importance of the molecular diffusivity coefficients, such as viscosity and species diffusivity, must not only enter in this description, but are likely to do so in a non-universal way.

It is interesting that transition to turbulence, at intermediate values of the Reynolds number, appears to be universal, whereas mixing in fully-developed turbulence, at high Reynolds numbers, does not.

7. Acknowledgements

The work described here is part of a larger program at Caltech to study mixing and chemically reacting turbulent flows and the result of the efforts, collaboration, and discussions of many people over the years. In the context of the material presented in this paper, I would specifically like to acknowledge the work and discussions with Paul L. Miller, on turbulent jet mixing, and Chris L. Bond, who recalculated many of the data points in Figs. 8 from the original measurements. This work was supported by the Air Force Office of Scientific Research, Grant Nos. 88–0155, 90–0304, and F49620–92–J–0290, and the Gas Research Institute Contract No. 5087–260–1467.

References

[1] Brown, G. L., and Roshko, A., "On Density Effects and Large Structure in Turbulent Mixing Layers," *J. Fluid Mech.* **64**, 775–816 (1974).

[2] Eckart, C., "An Analysis of the Stirring and Mixing Processes in Incompressible Fluids," *JMR* **VII**, 265–275 (1948).

[3] Dimotakis, P. E., "Two-Dimensional Shear-Layer Entrainment," *AIAA J.* **24**, 1791–1796 (1986).

[4] Aref, H., "Stirring by chaotic advection," *J. Fluid Mech.* **143**, 1–21 (1984).

[5] Ottino, J. M., *The kinematics of mixing: stretching, chaos, and transport* (Cambridge University Press, 1989).

[6] Rom-Kedar, V., Leonard, A., and Wiggins, S., "An analytical study of transport, mixing and chaos in an unsteady vortical flow," *J. Fluid Mech.* **214**, 347–394 (1990).

[7] Ottino, J. M., "Mixing, Chaotic Advection and Turbulence," *Ann. Rev. Fluid Mech.* **22**, 207–253 (1990).

[8] Kuznetsov, V. R., and Sabel'nikov, V. A., *Turbulence and Combustion* (Hemisphere Publishing, New York, 1990).

[9] Konrad, J. H., *An Experimental Investigation of Mixing in Two-Dimensional Turbulent Shear Flows with Applications to Diffusion-Limited Chemical Reactions*, Ph.D. thesis, California Institute of Technology (1976).

[10] Brown, G. L., and Rebollo, M. R., "A Small, Fast-Response Probe to Measure Composition of a Binary Gas Mixture," *AIAA J.* **10**, 649–652 (1972).

[11] Breidenthal, R. E., "Structure in Turbulent Mixing Layers and Wakes Using a Chemical Reaction," *J. Fluid Mech.* **109**, 1–24 (1981).

[12] Koochesfahani, M. M., and Dimotakis, P. E., "Mixing and chemical reactions in a turbulent liquid mixing layer," *J. Fluid Mech.* **170**, 83–112 (1986).

[13] Masutani, S. M., and Bowman, C. T., "The structure of a chemically reacting plane mixing layer," *J. Fluid Mech.* **172**, 93–126 (1986).

[14] Bernal, L. P., Breidenthal, R. E., Brown, G. L., Konrad, J. H., and Roshko, A., "On the Development of Three-Dimensional Small Scales in Turbulent Mixing Layers," *2nd Int. Symposium on Turb. Shear Flows* (Springer-Verlag, New York, 1980), 305–313 (1979).

[15] Bernal, L. P., and Roshko, A., "Streamwise vortex structure in plane mixing layers," *J. Fluid Mech.* **170**, 499–525 (1986).

[16] Roshko, A., "The mixing transition in free shear flows," *The Global Geometry of Turbulence* (Impact of nonlinear dynamics), NATO Advance Research Workshop, 8–14 July 1990, Rota (Cádiz), Spain (1990).

[17] Moser, R. D., and Rogers, M. M., "Mixing transition and the cascade to small scales in a plane mixing layer," *Phys. Fluids A* **3**, 1128–1134 (1991).

[18] Dimotakis, P. E., Miake-Lye, R. C., and Papantoniou, D. A., "Structure and Dynamics of Round Turbulent Jets," *Phys. Fluids* **26**, 3185–3192 (1983).

[19] Seitzman, J., Üngüt, A., Paul, P., and Hanson, R., "Imaging and Characterization of OH Structures in a Turbulent Nonpremixed Flame," 23rd Symposium (International) on Combustion/The Combustion Institute, 637–644 (1990).

[20] Dowling, D. R., and Dimotakis, P. E., "Similarity of the concentration field of gas-phase turbulent jets," *J. Fluid Mech.* **218**, 109–141 (1990).

[21] Miller, P. L., and Dimotakis, P. E., "Reynolds number dependence of scalar fluctuations in a high Schmidt number turbulent jet," *Phys. Fluids A* **3**, 1156–1163 (1991).

[22] Miller, P. L., *Mixing in High Schmidt Number Turbulent Jets*, Ph.D. thesis, California Institute of Technology (1991).

[23] Gilbrech, R. J., *An Experimental Investigation of Chemically-Reacting, Gas-Phase Turbulent Jets*, Ph.D. thesis, California Institute of Technology (1991).

[24] Gilbrech, R. J., and Dimotakis, P. E., "Product Formation in Chemically-Reacting Turbulent Jets," *AIAA* 30$^{\text{th}}$ *Aerospace Sciences Meeting*, Paper 92–0581 (1992).

[25] Hottel, H. C., "Burning in Laminar and Turbulent Fuel Jets," 4$^{\text{th}}$ Symposium (International) on Combustion (Williams and Wilkins, Baltimore, 1953), 97–113 (1952).

[26] Broadwell, J. E., "A Model of Turbulent Diffusion Flames and Nitric Oxide Generation. Part I," TRW Document No. 38515-6001-UT-00, EERC Final Report, PO No. 18889 (1982).

[27] Dahm, W. J. A., and Dimotakis, P. E., "Measurements of Entrainment and Mixing in Turbulent Jets," *AIAA J.* **25**, 1216–1223 (1987).

[28] Bilger, R. W., "Turbulent Flows with Nonpremixed Reactants," *Turbulent Reacting Flows* (Eds. P. A. Libby, F. A. Williams, *Topics in Applied Physics* **44**, Springer-Verlag, New York), 65–113 (1980).

[29] Kuo, K. K., *Principles of Combustion* (John Wiley, New York, 1986).

[30] Dimotakis, P. E., "Turbulent Free Shear Layer Mixing and Combustion," *High Speed Flight Propulsion Systems*, in *Progress in Astronautics and Aeronautics* **137**, Ch. 5, 265–340 (1991).

[31] Namazian, M., and Kelly, J. T., "Near-Field Instantaneous Flame and Fuel Concentration Structures," Twenty-Second Symposium (International) on Combustion/The Combustion Institute, 627–634 (1988).

[32] Dahm, W. J. A., Dimotakis, P. E., and Broadwell, J. E., "Non-premixed turbulent jet flames," *AIAA* 22$^{\text{nd}}$ *Aerospace Sciences Meeting*, Paper 84–0369 (1984).

[33] Weddell, D., *Turbulent Mixing in Gas Flames*, Ph.D. thesis, Massachusetts Institute of Technology (1941).

[34] Dowling, D. R., *Mixing in Gas Phase Turbulent Jets*, Ph.D. thesis, California Institute of Technology (1988).

[35] Mungal, M. G., and Dimotakis, P. E., "Mixing and combustion with low heat release in a turbulent mixing layer," *J. Fluid Mech.* **148**, 349–382 (1984).

[36] Mungal, M. G, Hermanson, J. C., and Dimotakis, P. E., "Reynolds Number Effects on Mixing and Combustion in a Reacting Shear Layer," *AIAA J.* **23**, 1418–1423 (1985).

[37] Frieler, C. E., *Mixing and Reaction in the Subsonic 2-D Turbulent Free Shear Layer*, Ph.D. thesis, California Institute of Technology (1992).

[38] Hall, J. L., Dimotakis, P. E., and Rosemann, H., "Some measurements of molecular mixing in compressible turbulent mixing layers," *AIAA* 22nd *Fluid Dynamics, Plasma Dynamics and Lasers Conference*, Paper 91–1719 (1991).

[39] Broadwell, J. E., and Breidenthal, R. E., "A simple model of mixing and chemical reaction in a turbulent shear layer," *J. Fluid Mech.* **125**, 397–410 (1982).

[40] Dimotakis, P. E., "Turbulent shear layer mixing with fast chemical reactions," US-France Workshop on *Turbulent Reactive Flows* (Springer-Verlag, New York, 1989), 417–485 (1987).

[41] Hall, J. L., *An Experimental Investigation of Structure, Mixing and Combustion in Compressible Turbulent Shear Layers*, Ph.D. thesis, California Institute of Technology (1991).

[42] Dimotakis, P. E., "On the convection velocity of turbulent structures in supersonic shear layers," *AIAA* 22nd *Fluid Dynamics, Plasma Dynamics and Lasers Conference*, Paper 91–1724 (1991).

[43] Miller, P. L., and Dimotakis, P. E., "Measurements of scalar power spectra in high Schmidt number turbulent jets," GALCIT Report FM92–3 (1992).

[44] Broadwell, J. E., and Mungal, M. G., "Large-scale structures and molecular mixing," *Phys. Fluids* A **3**(5), Pt. 2, 1193–1206 (1991).

[45] Wygnanski, I., and Champagne, F. H., "On transition in a pipe. Part I: The Origin of Puffs and Slugs and the Flow in a Turbulent Slug," *J. Fluid Mech.* **59**, 281–335 (1973).

[46] Coles, D., "The law of the wake in the turbulent boundary layer," *J. Fluid Mech.* **1**, 191–226 (1956).

[47] A turbulent boundary layer is characterized by three transverse scales, whose separation increases with increasing Reynolds number: the inner, viscous sublayer; the intermediate, log-law layer; and the outer, wake region layer. The integral displacement thickness was used here as the single scale in the definition of Reynolds number.

[48] Coles, D., "The Young Person's Guide to the Data," Proc. AFOSR–IFP–Stanford Conference *Computation of Turbulent Boundary Layers*, **II** (D. Coles & Hirst, eds.), 1–45 (1968).

[49] Collins, D. J., Coles, D. E., and Hicks, J. W., "Measurements in the Turbulent Boundary Layer at Constant Pressure in Subsonic and Supersonic Flow. Part I. Mean Flow," AEDC–TR–78–21 (1978).

[50] Liepmann, D., and Gharib, M., "The role of streamwise vorticity in the near-field entrainment of round jets," *J. Fluid Mech.* **245**, 643–668 (1992).

[51] Hammer, J. A., *Lifted Turbulent Jet Flames*, Ph.D. thesis, California Institute of Technology (1993).

[52] Roshko, A., "Perspectives on bluff body aerodynamics," 2nd *Int. Coll. on Bluff Body Aerodynamics*, Melbourne, Australia (1992).

[53] Sreenivasan, K. R., "On the scaling of the turbulent energy dissipation rate," *Phys. Fluids* **27**, 1048–1050 (1984).

[54] Jimenez, J., Wray, A. A., Saffman, P. G., and Rogallo, R. S., "The structure of intense vorticity inhomogeneous isotropic turbulence," *Studying Turbulence Using Numerical Simulation Databases — IV*, Proceedings, 1992 Summer Program (Center for Turbulence Research, NASA Ames & Stanford U.), 21–45 (1992).

[55] J. Jimenez has noted (private communication) an alternate possible explanation for the Reynolds number behavior of the scaled dissipation rate, α (Eq. 11), in

this flow, as well as in grid turbulence.[53] He notes the decrease in the energy spectrum wavenumber span, and, therefore, in its integral, u'^2, with decreasing Reynolds number. In particular, he suggests that scaling the dissipation rate, ε, with an outer flow speed, instead of the velocity rms, u', could account for the observed Reynolds number behavior of this quantity.

[56] Heslot, F., Castaign, B., and Libchaber, A., "Transitions to turbulence in helium gas," *Phys. Rev.* A **36**, 5870–5873 (1987).

[57] Castaign, B., Gunaratne, G., Heslot, F., Kadanoff, L., Libchaber, L., Thomae, S., Wu, X.-Z., Zaleski, S., and Zanetti, G., "Scaling of hard thermal turbulence in Rayleigh-Bénard convection," *J. Fluid Mech.* **204**, 1–30 (1989).

[58] Lathrop, D. P., Fineberg, J., and Swinney, H. L., "Turbulent flow between Concentric Rotating Cylinders at Large Reynolds Number," *Phys. Rev. Lett.* **68**, 1515–1518 (1992).

[59] Lathrop, D. P., Fineberg, J., and Swinney, H. L., "Transition to shear-driven turbulence in Couette-Taylor flow," *Phys. Rev.* A **46**, 6390–6405 (1992).

[60] Monin, A. S., and Yaglom, A. M., *Statistical Fluid Mechanics: Mechanics of Turbulence* **II** (Ed. J. Lumley, MIT Press, Cambridge, MA, 1975).

[61] Chapman, D. R., "Computational Aerodynamics Development and Outlook," *AIAA J.* **17**, 1293–1313 (1979).

[62] Saddoughi, S. G., "Local isotropy in high Reynolds number turbulent shear flows," *Annual Research Briefs – 1992* (Center for Turbulence Research, NASA Ames & Stanford U., Jan. 1993), 237–262 (1992).

[63] This calculation is discussed in Ref. 21, where, for the purposes of estimating diffusion-layer thicknesses (transition from high to low values of the diffusing scalar), half this estimate, *i.e.*, $\lambda_\nu \approx \pi/k_\nu \simeq 25\,\lambda_K$, was used.

[64] Friehe, C. A., Van Atta, C. W., and Gibson, C. H., "Jet turbulence: Dissipation rate measurements and correlations," AGARD Turbulent Shear Flows CP–93, 18.1–7 (1971).

[65] Jimenez, J., Martinez-Val, R., and Rebollo, M., "On the origin and evolution of three-dimensional effects in the mixing layer," Internal Rept. DA–ERO–70–G–079, Univ. Politec., Madrid, Spain (1979).

[66] Huang, L.-S., and Ho, C.-M., "Small-scale transition in a plane mixing layer," *J. Fluid Mech.* **210**, 475–500 (1990).